Single-Cell Transcriptomic Profiling of MASH-HCC Development

Authors
Emma A. Rørbeck, Helene Ægidius, Grzegorz Maciag, Mikkel Christensen-Dalsgaard, Michele Vacca, Michael Feigh, Henrik H. Hansen, Martin Rønn Madsen

Gubra, Hørsholm Kongevej 11B, Hørsholm, Denmark

Corresponding author
Emma A. Rørbeck - ero@gubra.dk

Background & Aim

Bulk RNA-sequencing has limited cellular-level insight into metabolic-associated steatohepatitis (MASH) and its progression to hepatocellular carcinoma (HCC) by masking rare and tumor-relevant populations. Here, we used single-cell transcriptomics to characterize liver cell-specific transcriptomic changes in the GAN DIO-MASH-HCC mouse, a gold-standard translational model of MASH-driven HCC. We built a comprehensive liver single-cell atlas spanning healthy, MASH, and MASH-HCC mouse models, including tumor and adjacent non-tumor regions, to define hepatocyte state transitions from healthy liver through MASH to HCC.

Methods

Male C57Bl/6J mice (n=5 per group) were fed chow (CHOW) or the obesogenic GAN diet for 48 weeks (GAN DIO-MASH) or 68 weeks (GAN DIO-MASH-HCC). Paired tumor (HCC tumor, HCC-T) and adjacent non-tumorous (HCC non-tumor, HCC-NT) samples were collected and dissociated into single cells and processed with the 10x Genomics GEM-X Flex 4-plex kit.

Conclusion

+ We obtained around 280,000 cells to build a comprehensive liver single-cell atlas
+ All major liver cell types were recovered in all study groups
+ Bulk CHOW, MASH, and HCC transcriptional programs are recovered at single-cell resolution
+ Hepatocytes display a continuous axis from healthy to HCC-associated states that can be partitioned into four segments with distinct gene programs
+ This atlas provides a framework to identify cell-state transitions and disease-associated programs during MASH-HCC progression

www.gubra.dk

1 The GAN DIO-MASH and GAN DIO-MASH-HCC models

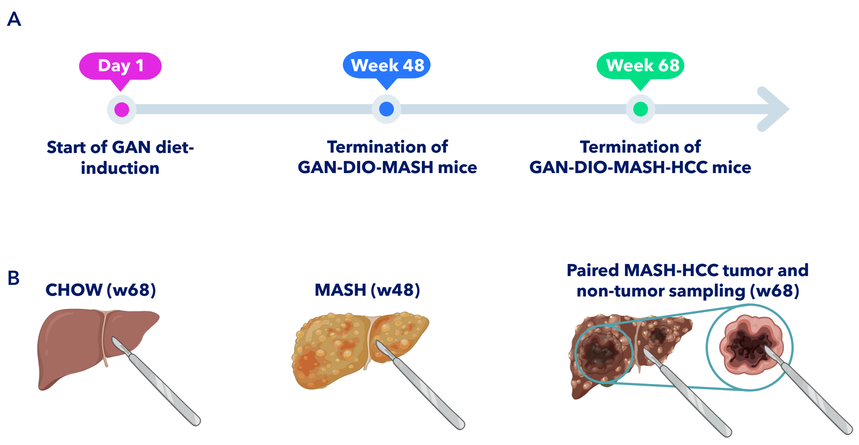

Figure 1. Study Overview of Mouse Liver Disease Models. (A) Timeline of GAN-diet induction for generation of the GAN DIO-MASH and GAN DIO-MASH-HCC mouse models. **(B)** Group overview: Age-matched lean chow-fed control mice (CHOW, w68, n=5), GAN DIO-MASH mice (w48, n=5), and GAN DIO-MASH-HCC mice (w68) with tumor-adjacent (n=5) and tumor samples (n=4). All collected samples were processed for single-cell RNA sequencing using the 10x Genomics GEM-X Flex Kit.

2 Hepatocellular atlas of the GAN DIO-MASH-HCC mouse

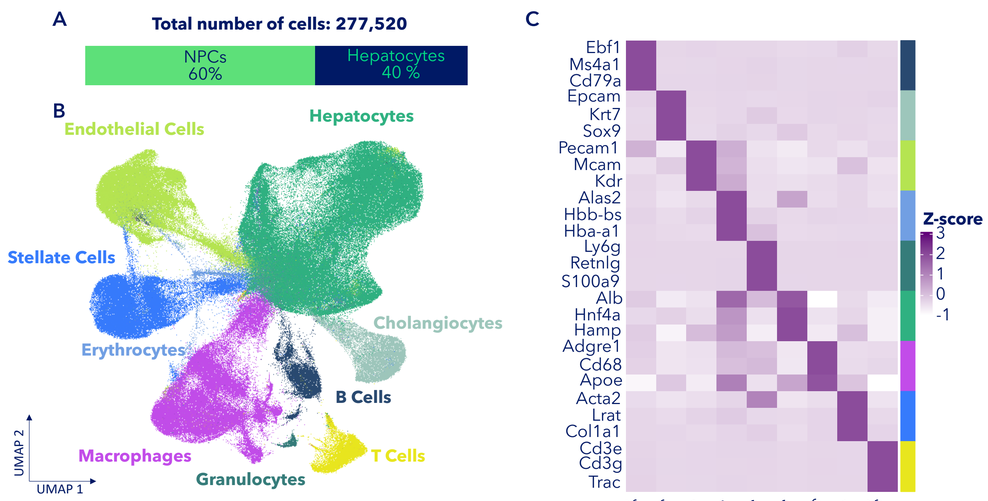

Figure 2. A comprehensive cellular atlas of healthy and MASH-HCC liver (A) Distribution of non-parenchymal cells (NPCs) and hepatocytes. **(B)** Uniform manifold and approximation projection (UMAP) projection of all ~280,000 cells colored by annotated cell type. **(C)** Heatmap of average expression (z-score) for selected marker genes across cell types.

3 Cell-type distribution during disease progression

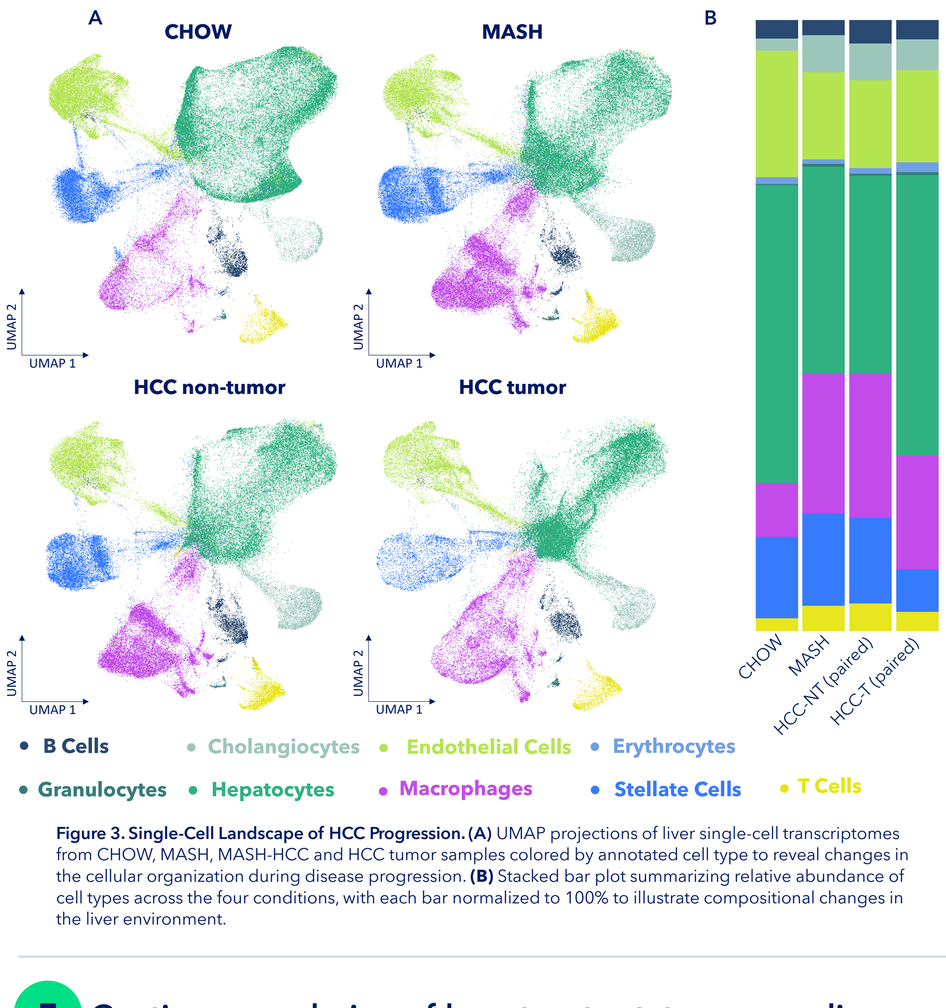

Figure 3. Single-Cell Landscape of HCC Progression. (A) UMAP projections of liver single-cell transcriptomes from CHOW, MASH, MASH-HCC and HCC tumor samples colored by annotated cell type to reveal changes in the cellular organization during disease progression. **(B)** Stacked bar plot summarizing relative abundance of cell types across the four conditions, with each bar normalized to 100% to illustrate compositional changes in the liver environment.

4 Bulk CHOW, MASH, and HCC clusters at single-cell resolution

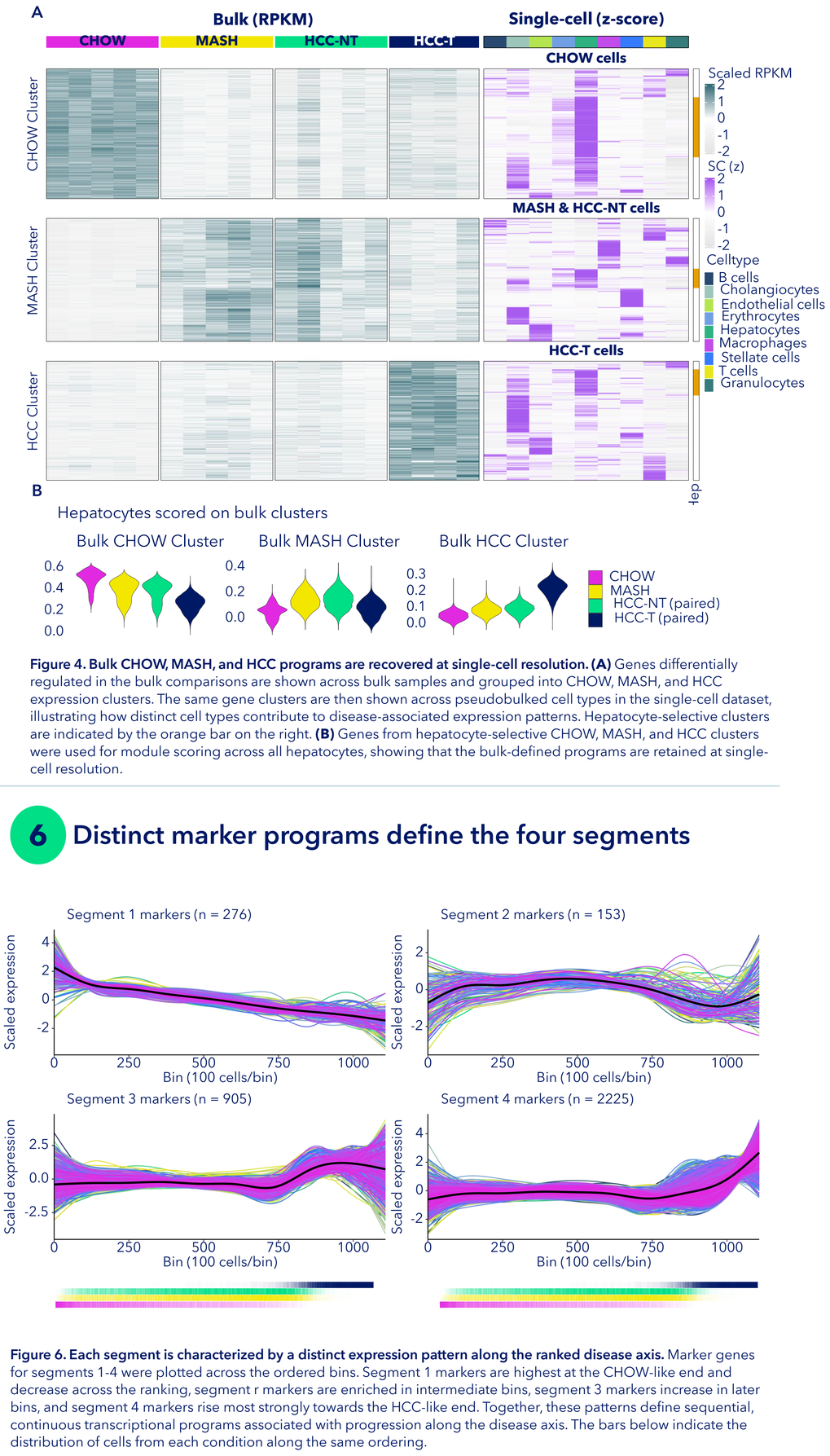

Figure 4. Bulk CHOW, MASH, and HCC programs are recovered at single-cell resolution. (A) Genes differentially regulated in the bulk comparisons are shown across bulk samples and grouped into CHOW, MASH, and HCC expression clusters. The same gene clusters are then shown across pseudobulked cell types in the single-cell dataset, illustrating how distinct cell types contribute to disease-associated expression patterns. Hepatocyte-selective clusters are indicated by the orange bar on the right. **(B)** Genes from hepatocyte-selective CHOW, MASH, and HCC clusters were used for module scoring across all hepatocytes, showing that the bulk-defined programs are retained at single-cell resolution.

5 Continuous ordering of hepatocyte states across disease

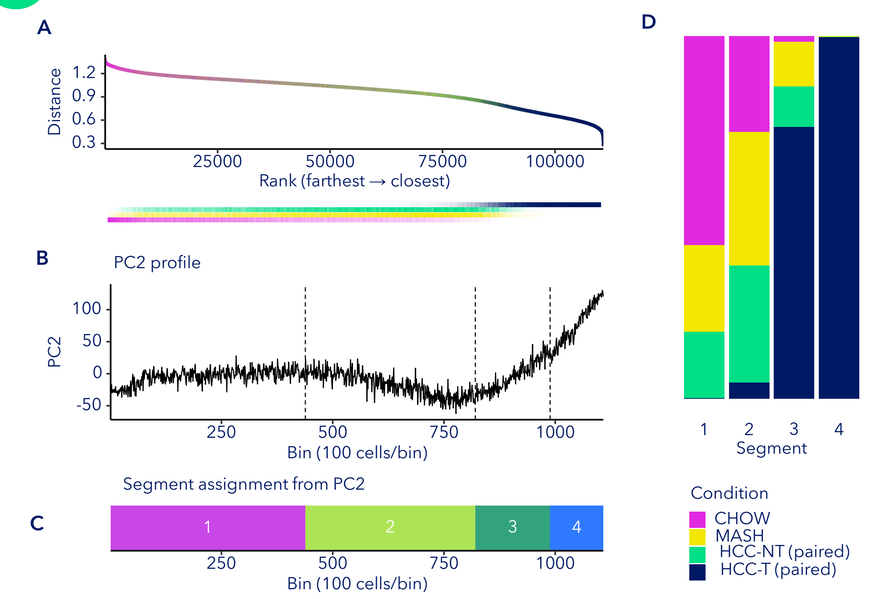

Figure 5. Hepatocytes were ordered by proximity to the HCC state and partitioned into four segments. (A) 3D embedding was generated from the CHOW, MASH, and HCC module scores for each hepatocyte, and the distance from each cell to the HCC vertex was used to rank cells from farthest to closest to the HCC state. The density bar below indicates the distribution of conditions across this ranking. **(B)** Ranked cells were grouped into bins of 100 cells, and PCA of the binned expression matrix identified the 2nd component (PC2) capturing the transition from healthy to malignant states. This profile was segmented using slope into four segments, seen in **(C)**. **(D)** The relative abundance of CHOW, MASH, HCC-NT, and HCC-T cells within each segment is shown.

6 Distinct marker programs define the four segments

Figure 6. Each segment is characterized by a distinct expression pattern along the ranked disease axis. Marker genes for segments 1-4 were plotted across the ordered bins. Segment 1 markers are highest at the CHOW-like end and decrease across the ranking, segment r markers are enriched in intermediate bins, segment 3 markers increase in later bins, and segment 4 markers rise most strongly towards the HCC-like end. Together, these patterns define sequential, continuous transcriptional programs associated with progression along the disease axis. The bars below indicate the distribution of cells from each condition along the same ordering.